Learning Seed Placements and Automation Policies for Polyculture Farming with Companion Plants

Yahav Avigal[1], Anna Deza[1], William Wong[1], Sebastian Oehme[2], Mark Presten[1], Mark Theis[1]
Jackson Chui[1], Paul Shao[1], Huang Huang[1], Atsunobu Kotani[1], Satvik Sharma[1], Rishi Parikh[1], Michael Luo[1]
Sandeep Mukherjee[1], Stefano Carpin[3], Joshua H. Viers[4], Stavros Vougioukas[5] and Ken Goldberg[1]

***Abstract*— Polyculture farming is a sustainable farming technique based on synergistic interactions between differing plant types that make them more resistant to diseases and pests and better able to retain water. Reduced uniformity can reduce use of pesticides, fertilizer, and water, but is more labor intensive and more challenging to automate. We describe a scaled physical testbed (1.5m×3.0m) that uses a high resolution camera and soil sensors to monitor polyculture plants to facilitate tuning of plant growth, companion effects, and irrigation parameters for a first-order garden simulator. We use this simulator to develop a novel seed placement algorithm that increases coverage and diversity, and a learned pruning policy. In simulation experiments, the seed placement algorithm yields 60% more coverage and 10% more diversity than random seed placement and the learned pruning policy runs 1000X faster than a procedural lookahead policy to achieve high leaf coverage and plant diversity on adversarial gardens that include plant species with diverse growth rates. These models and policies provide the groundwork for a fully-automated system under development. Code, datasets and supplementary material can be found at https://github.com/BerkeleyAutomation/AlphaGarden/.**

I. Introduction

Polyculture farming, where multiple plant species are intercropped simultaneously and in close proximity, is a form of agricultural cultivation used for centuries that has been shown to enhance pest control, reduce weeds, limit soil erosion, and provide better use of light, water and soil nutrients [1], [2], [3], [4]. It is known that specific mixtures of cultivted plant species can result in higher overall yield [5]. Examples of mutually beneficial polycultures developed prior to industrial agriculture include maize-bean mutualisms, where maize provides a structural scaffold for the nitrogen-fixing leguminous vines [6], and intercropping of deep rooted native shrubs into grain cultivation, which improves water availability in arid regions [7]. More contemporary examples include shade-grown coffee, where species diverse agroforestry practices that can included cacao and banana intercropping provide not only canopy shade for coffee, increasing yields, but also provides needed habitat for birds, butterflies and other species [8]. Monoculture farming, as typically practiced in large-scale, industrial applications, is often characterized by heavy agrichemical inputs, such as chemical fertilizers and pesticides [9], [10], and increased vulnerability to disease and pestilence. The lack of long-term sustainability of industrial agriculture [11], and its implications for human food security, has sparked renewed interest in polyculture [12], [13], [14].

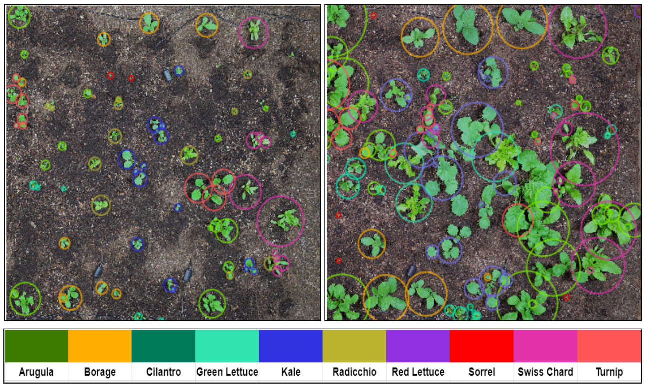

Fig. 1: **Tuning Plant Simulation Parameters Using the Physical Testbed**. Using seeds from 10 edible plant species the seed locations were computed with a seed placement optimization process that leverages companion plants relationships to increase plant coverage and diversity. **Left:** Garden at day 17. **Right:** Garden at day 25. Plant circles as shown are predicted using the algorithm described in Section III(c).

One drawback is that polyculture farming requires more human labor than monoculture farming due to variations in germination times and growth rates.

We are exploring the use of a robot with a learned control policy to automate polyculture farming and assist - not replace - farm workers. Due to the large time constants in nature, learning such a policy through real world experiments could require many years. In prior work we introduced AlphaGardenSim [12], an efficient, open access, first order simulator for polyculture farming. The simulator models inter-plant dynamics through competition for resources, but did not take into account relations between specific plant species. In this paper, we explore inter-plant influence, seed placements, irrigation and pruning. This paper makes 4 contributions:

1) AlphaGardenSim 2.0, an open-source polyculture plant simulator tuned with real world measurements from a physical testbed.
2) Significant extensions to the AlphaGardenSim 1.0 simulator to model companion plant effects.
3) A seed placement algorithm that uses companion plant

[1] The AUTOLab at UC Berkeley (automation.berkeley.edu) {yahav_avigal, goldberg} @berkeley.edu
[2] Department of Electrical and Computer Engineering, TU Munich sebastian.oehme@tum.de [3] School of Engineering, UC Merced scarpin@ucmerced.edu [4] Environmental Systems, School of Engineering, UC Merced jviers@ucmerced.edu [5] Biological and Agricultural Engineering, UC Davis svougioukas@ucdavis.edu

relations to generate seed placement plans that yield high coverage and plant diversity.

4) A supervised-learning policy that optimizes plant coverage and diversity over a short horizon.

II. Related Work

In 1995, Goldberg et al. [15], [16] presented the Telegarden, an art installation that allowed anyone on the Internet to interact with a garden by planting and watering plants. Wiggert et al. [17] created a testbed that enables real-time data collection for precision irrigation based on observed plant growth and water stress. Fernando et al. [18] use a greenhouse to evaluate mobile robot monitoring of plant health and soil moisture. We build on these prior works by creating a robot-assisted garden which also facilitates real-time data collection for automated control.

Few simulators include the option to model growth of multiple species in a garden [19]. Simulators such as DSSAT [20] and AquaCrop [21] simulate large-scale monoculture farms. Whitman et al. [22] use Gaussian processes to predict weed growth across a farm. Our prior work, AlphaGardenSim [12] simulates a polyculture garden using first order models of single plant growth, simulating inter-plant dynamics and competition for water and light, but was prone to error when the plants have significantly distinct germination times, growth rates, and poor initial placements.

Gou et al. [23] propose a model to simulate the growth of two species in a strip-relay intercropping system. They propose a method to calibrate the plant specific parameters given observed field data. However, this model only takes into account light competition, assuming that irrigation is sufficient. The model allows for analysis of different seed placements on plant growth but restricts to the strip intercropping environment. Tan et al. [24] build on Gou et al. and include the effects of water acquisition suggesting that plants use land and water more efficiently in intercropping. However, their model does not allow for exploring spatial patterns beyond the strip-relay setting and limits to two species.

Both Gou et al. [23] and Tan et al.[24] do not make explicit use of plant characteristics to define plant inter-relations. Yu [25] use a simulated functional-structural plant model to investigate which plant traits contribute to complementary relationships and the effects of different plant placements, assuming irrigation provides sufficient water for all plants.

These simulators consider the polycultural setting, but they either do not model the light and water competition simultaneously and/or are limited by the placement geometry that they consider. We present extensions to AlphaGardenSim to incorporate plant relationships and consider inter-plant cooperation.

III. Plant Phenotyping

We fabricated a 1.5×3m garden bed in the UC Berkeley greenhouse and mounted a commercial FarmBot gantry robot system [26] to tune and test AlphaGardenSim on real plants. We use a high-resolution overhead camera that has a full view of the garden, soil moisture sensors and an automated pruning tool. A uniform and nutrient rich soil was used to reduce stochastic effects in nutrient availability.

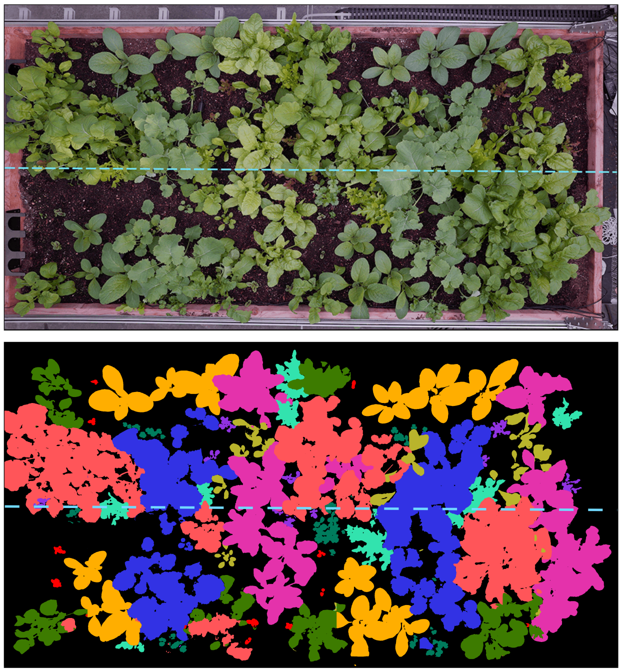

	⬛	🟦	🟪	🟥	🟩	🟧	🟩	🟩	🟥	🟨	🟪
Name	unknown / soil	kale	swiss chard	turnip	arugula	borage	green lettuce	cilantro	sorrel	radicchio	red lettuce
% Coverage	48.4	11.8	10.1	9.7	7.4	7.0	1.7	1.0	0.3	0.2	0.1
Baseline IoU	0.88	0.78	0.81	0.55	0.40	0.82	0.72	0.46	0.70	0.13	0.39
IoU with augmentation	0.92	0.92	0.93	0.81	0.72	0.95	0.87	0.71	0.76	0.57	0.65

Fig. 2: **Learned Plant Segmentation Model**. The figures above (from top to bottom) show an overhead image from October 6, 2020, and the classifier output from the network with augmented data. The overhead image is split in half as shown by the blue line. The top half is for training while the bottom half is for testing. Below, the table shows how much of the garden is covered by each plant and its respective IoU score based on the bottom half only. By adding augmented data, the model was able to more accurately classify unseen leaves when compared to the baseline with no augmented data. Low IoU for radicchio and red lettuce is consistent with a low percent of coverage.

a) Camera: The digital camera, mounted 2m above the garden bed, is a Sony SNC-VB770 and takes images every 24 hours. Its 35 mm sensor has a maximum 4240×2832 resolution (1.4x higher than 4K) image mode, and a 3840×2160 (4k) video mode. We also selected a 20 mm focal length Sony lens designed for SLR-type mirror-less cameras of comparable quality. Its optical design minimizes aberrations and distortion, providing a clear detailed image with no fishseye effect.

b) Leaf Segmentation: See Fig. 2. We implemented semantic segmentation to study plant canopy coverage. To estimate the canopy distribution from overhead images, we predict a plant type, or "unknown," for each pixel in the overhead image, using the UNet [27] architecture with a ResNet34 [28] backbone pre-trained with weights from ImageNet [29] data. We then use two 2,000×3,780 and one 1,630×3,478 overhead images taken of the garden on September 26, September 30, and October 6, 2020, with hand-labeled ground truth masks of plant phenotypes, and divide each image into a top half and bottom half as shown in Fig. 2. We extract 48 512×512 patches from the top half for training. We then modifwey these patches through actions such as shearing, shifting, and scaling.

A key challenge is generalizing across all garden days and plant life stages. To address this, we extract individual leaves from October 1 to 22, 2020 to get samples of various sizes, plant health, lighting, and texture. We augment the dataset by overlaying individual leaves on top of each patch. By varying the position and pose of each augmented leaf, we create 100 patches of training images from a single overhead image. This additional augmented data improves network robustness as shown in Fig. 2.

We train using 3,180 patches, 1,500 of them from augmented data, and 1680 from the original data. Training uses categorical cross-entropy loss over 100 epochs and utilizes a 75-25 train-validation split. The output is a 512×512×11 array, with 11 softmax likelihoods, representing ten plant phenotypes (or ”unknown”). We classify a pixel by choosing the largest likelihood, and create a predicted mask for an overhead image by combining the classified 512×512 patches. Fig. 2 shows the network's prediction on the bottom half of the image from October 6, 2020, which is unseen to the network. When evaluated, the model has a mean IoU of 0.80. The model performs well in identifying plant types with high coverage, but has lower accuracy in plants that are not common in the overhead image.

c) Converting Segmentation Masks to Circles: See Fig. 1. To convert the pixel-wise segmentation masks into the circular model used in AlphaGardenSim [12] we track plant centers and radii. We define the plant center as the average over all pixel locations in the plant's segmentation mask. We define the radius as the distance from the new center to the farthest point on its contour and note that although the seed locations are known, plant centers change over time due to phototrophy [30] and irrigation [31]. Given the centers and radii of all plants on day $t-1$ as a prior, we use three heuristics to guide the circles update on day t: the previous center, a minimum-, and a maximum-radius estimate. The radius estimates are computed by finding the maximal and minimal observed radius per day for each plant type using real world measurements as described in Section V. We use a breadth-first-search (BFS) algorithm, traversing radially outward to update each of the circles. The BFS terminates when either the max radius estimate is achieved or the percentage of new pixels discovered during the previous two iterations is lower than a threshold (1%). After termination, the new center is the center of mass of the pixels within the circle and the new radius is the distance from the termination point to the center, as shown in Fig. 1.

IV. Irrigation Model

We utilized six TEROS-10 [32] volumetric water content (VWC) soil sensors connected to a ZL6 Data Logger [32] to measure soil moisture. The first set of experiments refined the irrigation application parameter, $a(x, y, t)$, the amount of irrigation applied at point (x, y). We identified the flow rate from the FarmBot nozzle to be 0.083 L/s. The area of influence from the nozzle is a circle of 0.04m radius.

We then used the soil moisture sensors to determine radial flow. By watering at varying distances spanning from 0.04m to 0.10m from the center of a soil moisture sensor, we determined a model as follows: beginning outside of the 0.04m radius, the water gain is roughly half that when compared to water gain within the radius. This trend continues each additional 0.01m away from the center watering point up until 0.09m. Let $w(x, y)$ be the VWC centered at at point (x, y) in the garden. Thus, $\Delta w(x_d, y_d) = (1/2)^d * gain$ where d is distance measured in 0.01m outside of the 0.04m radius, (x_d, y_d) is a point $d + 0.04\mathrm{m}$ away from (x, y), and $gain$ is the moisture gain for soil directly under the nozzle.

We studied changes in soil moisture content from irrigation procedures to tune the local water loss parameter, d. Using soil moisture over time curves produced from irrigation experiments in which we watered at different frequencies, we identified a water gain and water loss period post watering event. In the water loss period, the change in soil moisture over time t in hours fits nicely to a weighted, negative logarithmic decay: $\Delta w = -0.01675 \cdot \ln t$.

Furthermore, we used the soil moisture sensors to tune the prior soil moisture content parameter, $w(x, y, t-1)$. Here, the quantity that is important for identifying real world irrigation policies is the soil's specific maximal VWC which describes how much moisture the soil can store [33]. By saturating several different samples of soil that we used in the physical testbed, we discovered the max VWC of our soil to be around 0.3, and capped the $w(x, y, t-1)$ accordingly.

Through the execution of irrigation and soil moisture experiments in the physical testbed, we made adaptations to parameters based on Richards equation for soil moisture dynamics used in [12]:

$$w(x, y, t) = \max(w(x, y, t-1) - d + a(x, y, t) - U(x, y, t), 0)$$

V. Growth Analysis

The standard agriculture parameters that dictate growth are germination time, maturation time, and maximum radius. Individual plants also depend on the light, water, the plant starting radius and height, and the number of days the plant remains in its growth phase versus its wilting phase. The starting radius and height in the simulation and the number of days in which a plant grows before wilting are sampled from a normal distribution centered around the values defined above.

Through the use of overhead photos of the physical testbed, we can measure each plant's radial growth. Similar to how growth is modeled in our simulator, we annotated every plant with a point at its center and a point at its outermost radius in an image from every day since seeding. We then made a rough conversion of pixel coordinates to real world coordinates in cm. These coordinates were then used to find plant radius in cm for that day.

By analyzing the growth of the one-hundred-twenty plants in the garden over 46 days, and averaging the growth of a

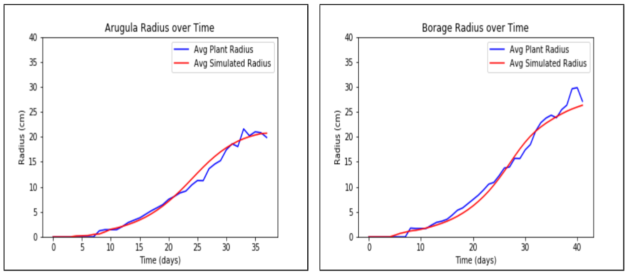

Fig. 3: Plots of growth curves, radius (cm) over time (days), for both simulated and real world plants. Borage was occluded by other plants after day 40. Arugula was occluded starting on day 35. The blue curve is real world radius. The red logistic curve is simulated radius from AlphaGardenSim.

Plant Type	g_0	g_1	m_0	m_1	r_1	c_1	$c(35)$	$e(35)$
Borage	7	7	49	55	60	0.09	3107	6.61
Kale	3	7	62	55	65	0.10	7450	5.41
Swiss Chard	7	7	53	50	47	0.11	5536	9.93
Turnip	3	7	42	47	53	0.11	3961	10.04
Green Lettuce	7	9	43	52	27	0.08	232	7.46
Arugula	5	8	45	52	40	0.10	1133	5.50
Sorrel	7	15	53	70	8	0.08	59	9.58
Cilantro	7	10	53	65	20	0.09	23	10.76
Red Lettuce	5	12	45	50	28	0.09	10	11.61
Radicchio	5	9	83	55	53	0.09	53	9.28

TABLE I: Growth Analysis: Where g_0 (days) is original germination time, g_1 (days) is tuned germination time, m_0 (days) is original maturation time, m_1 (days) is tuned maturation time, r_1 is radial growth potential, c_1 is radial growth rate, $c(35)$ (cm^2) is the simulated canopy coverage on day 35, and $e(35)$ (cm) is the mean absolute error on day 35 between simulated and average real world radius. Original values were taken from published plant tables [34]. Growth time is found by subtracting g_1 from m_1. Sorrel not only germinated later than other plants, but also had a growth potential and growth rate that was minuscule compared to other plants in the physical testbed.

plant with others of its same species we created a new growth function in AlphaGardenSim:

$$r(t) = \frac{r_1}{1 + r_1 \cdot e^{-c_1 t}}$$

where r_1 is the plant's radial growth potential, which controls how large the plant will grow, and c_1 is the plant's radial growth rate, which controls how fast the plant will grow. Both values were fitted using measurements from the garden, as shown in Fig. 3. The growth parameters of all ten plant species were tuned in the simulator to match real measured values, as shown in Fig I. The mean absolute error (MAE) between the simulated plants and physical testbed plants is displayed in Table I, along with growth parameters. It should be noted that we observe substantial plant overlap by day 35, and after this day it was difficult to identify a plant's outermost radius. Thus, the MAE is taken on day 35 rather than day 46.

VI. Companion Planting

Companion planting is an ancient technique of polyculture where mutually beneficial plant types are placed in proximity to each other. A positive or negative relationship between companion plants can exist due to above and below ground interactions [35], [36], [37]. Above ground includes physical environment changes such as providing shade, protecting against weather damage, and supplying structural support. Below ground interactions include providing nitrogen which fertilizes the soil, root-root activity and allelopathy, which occurs when a plant releases toxic chemicals that inhibit growth of other plants. While some crops such as grain and fruit trees require uniform spacing for optimal growth or harvesting, some such as leafy greens do not and can take advantage of large seed beds such as the one in the physical testbed. This motivates a method to find a garden seed placement that exploits plant relationships, which can lead to different yields and more or less efficient use of resources [38], [39].

a) Modeling Companionship: Consider a garden with N seeds: $\{s(1), \cdots, s(N)\}$. Denote $\mathcal{K}$ as the set of plant types in the garden, $p(i) \in \mathcal{K}$ as the plant type of seed i, and $l(i) = (x_i, y_i)$ as the location of seed i. Let $r_k^{\max}$ denote the expected maximal radius of plants of type k. To model plant interrelationships we use the plant relationship matrix $\mathbf{C} \in \mathbb{R}^{|\mathcal{K}| \times |\mathcal{K}|}$. $\mathbf{C}_{i,j}$ stores a number that describes the level of companionship between plants of type i and j, which are not necessarily symmetric. In simulation, $\mathbf{C}$ is used to calculate a local plant specific companionship factor c. For a given plant i,

$$c_i = \sum_{j \in [1, \cdots, N], j \neq i} \frac{\mathbf{C}_{p(i),p(j)}}{\|l(i) - l(j)\|_2^2}$$

The strength of the companionship decays as the distance between them grows.

In AlphaGardenSim 2.0, each plant's daily radius grows according to a factor $\tilde{G}$, determined by the local water and light resources and competition. The effects of companionship are modelled by a change to the growth value in the simulator. The growth value is updated to be $G = \tilde{G} \cdot c$.

The $\mathbf{C}$ matrix was determined using the one-hundred and twenty annotations provided by analyzing growth rates in the physical testbed. Plants in the same relative location on each side of the garden were compared to one another as well as the average growth; if the same plant on both sides exhibited either exaggerated growth or stunted growth, the neighbors were noted and assigned positive or negative scalar values, respectively, to indicate companionship between plants. These scalar values were then tuned to minimize the MAE between simulated and real world individual plants.

b) Seed Placement: Given two plants, the larger their relationship score the closer they would prefer to be. Then for a garden of width W and height H with N seeds, the following problem is solved to compute seed coordinates (x_i, y_i) for every plant i:

$$\begin{aligned} \max \quad & \sum_{i,j \in [N], i \neq j} \frac{\mathbf{C}_{p(i),p(j)}}{\|l(i) - l(j)\|_2^2} \\ \text{s.t.} \quad & r_{p(i)}^{\max} \leq x_i < W - r_{p(i)}^{\max} && \forall i \in [N] \\ & r_{p(i)}^{\max} \leq y_i < H - r_{p(i)}^{\max} && \forall i \in [N] \\ & \alpha(r_{p(i)}^{\max} + r_{p(j)}^{\max}) \leq \|l(i) - l(j)\|_2 && \forall i \neq j \in [N] \end{aligned}$$

The objective is to seed plants with a positive symbiotic relationship close to each other and vice versa when the relationship is negative. The first and second constraints ensure that seed locations are within the garden boundaries.

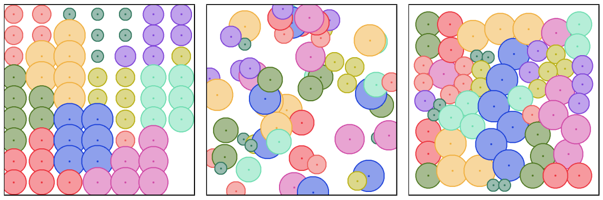

(a) Greedy (b) Random (c) Optimized

Fig. 4: **Left:** Seed placement achieved by greedy neighbourhood swap algorithm which ignores plant maximal radii, only taking into account companionship scores. This produces an artificial looking garden with limited interactions between plants of different species. **Middle:** Random seed placement, producing a sparse garden with seeds too close together, limiting the achievable coverage and diversity due to competition. **Right:** Seed placement obtained by using the optimization described in Section V. Small clusters of plants in irregular shapes are spread across the garden, allowing for a variety of interactions between different plant species.

Finally the last constraint ensures that plant radii do not overlap more than $100(1-\alpha)$ percent. α is a parameter in $[0,1]$ that specifies the maximal level of overlap between plants. A larger α results in more plants overlapping and thus interacting with each other. However if α is too large, plants tend to create very tight clusters of companion species, resulting in a difficulty for these plants to grow and a limited coverage. In this case, the negative effects of competition between neighbouring plants outweigh the benefit brought by the proximity of companion plants. To set α for a 150cm $\times$ 150cm garden with 10 species and 6 seeds of each type, gardens were generated with $\alpha \in [0.5, 0.55, 0.6, 0.65, 0.7, 0.75, 0.8, 0.85, 0.9, 0.95, 1.0]$. Each garden was simulated 5 times and $\alpha = 0.8$ producing the highest average coverage and diversity was selected. The resulting seed placement is shown in Fig. 4.

VII. Pruning and Irrigation Policies

a) Analytic Automation Policy: In prior work [12], we presented an analytic automation policy, Fixed Pruning, with hand tuned parameters. For $D(k)$, a set of k plant types available in the garden, the policy observes the local canopy coverage, plant health, and soil moisture levels defined by a $\frac{H}{10} \times \frac{W}{5}$ sector of the garden. In addition, the policy observes $\mathbf{p}(k,t)$, the global population in the garden as a distribution over point types D. It applies one of four actions in each sector: irrigate, prune, irrigate and prune, or null. When pruning, the policy creates $5{\times}5\text{cm}$ pruning window centered around a target plant, simulating the inaccuracy of a pruner, and reduces the radii of all plants visible in the window by a fixed ratio U. To decide to prune, the policy checks if the proportion of any plant type in the pruning window is higher than a uniform threshold. To evaluate the policy's performance, we compute the average of canopy coverage, plant diversity and water usage across days 20 to 70. We focus on these 50 days since during these days both the fast and the slow growing plants are in a growing stage.

However, as described in Section VIII(b), experiments suggest that Fixed Pruning struggles to manage plants with significant differences in germination times, maturation times and max radii.

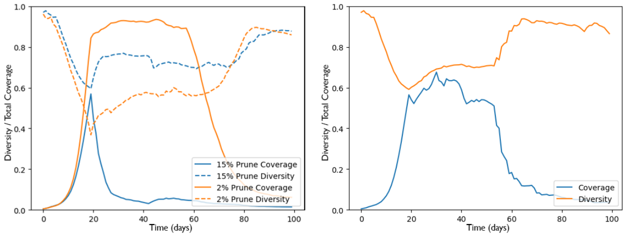

(a) Fixed Pruning (b) Variable Pruning

Fig. 5: **Left:** Simulation results for Fixed Pruning with fixed prune levels of 15% and 2%. 15% prune level achieves good diversity but low coverage. 2% prune level is the opposite. **Right:** Variable Pruning on gardens over 100 days with the fast and slow growing plant types from Table II. Favoring coverage initially, the policy uses variable pruning levels to achieve an average coverage of 0.51. As Variable Pruning begins to value diversity more, it uses higher prune rates beyond day 50 to achieve good coverage and diversity.

Plant Type	Germination (days)	Maturation (days)	Max Radius (cm)
Fast growing	9.8	99.4	140.4
Slow growing	25.6	156.0	42.4

TABLE II: Average germination time, maturation time, and max radii of 5 fast and 5 slow growing plant types. We vary germination times, maturation times and max radii of plants to identify combinations, such as the one in the table, on which the analytic policy achieves significantly lower coverage, as shown in Fig. 5(a).

b) 1-Step Lookahead Policy: To address this limitation, we introduce Variable Pruning, a policy which dynamically selects a pruning level $U(t) \in \mathcal{U}$ for each day t from a discrete set of six pruning levels $\mathcal{U}$, by taking a 1-step lookahead, simulating the potential coverage c_{u_i} and diversity values d_{u_i} that would result from choosing pruning level $u_i \in \mathcal{U}$ on the current state of the garden. With the simulated results, the policy uses tunable weights w_c and w_d to favor either coverage or diversity at different times of the growing period. To favor coverage during early growing periods and diversity later on, we set $w_c = 1 - \frac{\tilde{t}}{50}$ and $w_d = \frac{\tilde{t}}{50}$ where $\tilde{t} = t - 20$, starting to affect after the prune delay ends and lasting for 50 days until day 70. To favor diversity early and coverage later, the weights are swapped. The policy uses a weighted sum to determine which pruning level is preferable for day t:

$$U(t) = \max_{u_i \in \mathcal{U}} (w_c \cdot c_{u_i} + w_d \cdot d_{u_i})$$

Once Variable Pruning chooses $U(t)$, it uses Fixed Pruning to determine actions for the sectors observed each day to maximize both diversity and coverage.

c) Learned Policy: The computation time of Variable Pruning however, increases with $|\mathcal{U}|$. Each day, Variable Pruning must run the simulator $|\mathcal{U}|$ more times than Fixed Pruning. To reduce the computational cost of Variable Pruning, we train a deep supervised learned policy, Learned Pruning, mapping prune level $U(t)$ demonstrations to full garden observations as depicted in Fig. 6.

VIII. Simulation Experiments

a) Seed Placement: We compare the coverage and diversity achieved on two types of gardens shown in Fig. 4: (i) random seed placement and (ii) optimized seed placement using six seeds for each of the ten plant types in Table I. Averaging over 10 simulations each, the optimized garden

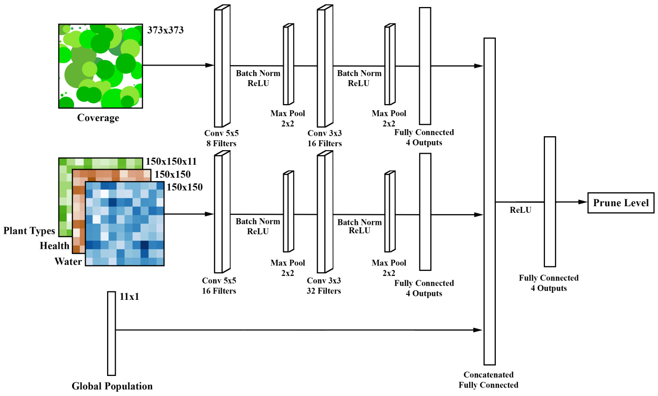

Fig. 6: Learned Pruning Policy. A deep CNN with 18,244 parameters. The network takes three inputs: an RGB image of the full garden, the distribution of plant types, plant health and water levels, and the global population distribution with soil. A prune level is predicted for the input observation.

achieves over 60% more coverage and 10% more diversity than the randomly seeded gardens.

b) Fixed Pruning Performance: To illustrate the shortcomings of Fixed Pruning on plants with different germination times, maturation times and max radii, we simulated 2 fixed pruning policies, with 15% and 2% pruning levels respectively, on a garden with 100 plants, 10 plants from each of the 10 plant types in Table II where faster growing plants grow 2X-20X faster than slower ones. Illustrated in Fig. 5(a), since 5 species grow significantly faster than the other 5, garden diversity rapidly drops during days 10 to 20. To achieve uniform plant diversity, 15% heavily prunes the faster plants to match the size of the slower growing plants resulting low coverage. In contrast, 2%'s pruning fails to keep up with the fast growing plants, resulting in lower plant diversity compared to 15%.

c) Variable Pruning Performance: To compare Fixed Pruning and Variable Pruning, we evaluate their performances on two sets of 10 plant types. We initialize $150 \times 150\text{cm}$ sized gardens with 100 plants each sampled with replacement from the plant types. For Variable Pruning, we set $w_c = 1 - \frac{\tilde{t}}{50}$ and $w_d = \frac{\tilde{t}}{50}$ to favor coverage early and diversity later. After experimenting with different pruning levels, we provided Variable Pruning these pruning levels: $\mathcal{U} \in (5\%, 10\%, 16\%, 20\%, 30\%, 40\%)$. The first set of plants are from Table I and have similar growth parameters. From experiments, we found that a fixed prune level of 15% for Fixed Pruning leads to the highest coverage and diversity values on the plant set. Results averaged across 20 test gardens with random seed placements are summarized in Table III. While Variable Pruning achieves higher coverage due to its ability to favor coverage over diversity during early growing periods, both policies achieve similar diversity and water use. This is expected as a fixed prune level is able to handle plant types with similar growth patterns.

Using the same parameters for both policies, we evaluate their performances on the fast and slow growing species from Table II. Results are presented in Table III and Fig. 5. Fixed Pruning achieves low coverage on these gardens, killing the plants at the beginning of the growing period. The high diversity achieved afterwards represents a uniform but empty garden. Variable Pruning, by favoring coverage early on, initially uses a small prune level of 5%. As w_d increases and w_c decreases over time, the policy shifts to favoring diversity and uses higher prune levels between 10% and 40%. As a result, Variable Pruning achieves high coverage and diversity.

Metric	Fixed	Variable	Learned
Avg coverage	0.38	**0.44**	-
Avg diversity	**0.92**	0.91	-
Avg water use	0.06	0.06	-
Avg coverage	0.24	**0.51**	0.50
Avg diversity	**0.77**	0.73	0.73
Avg water use	0.08	0.08	0.08
Computation time (seconds)	-	987.56	**0.92**

TABLE III: Policy evaluations of Fixed Pruning, Variable Pruning and Learned Pruning averaged across 20 test gardens. **Top 3 rows:** use the 10 plant types from Table I. **Bottom 4 rows:** use the plant types from Table II.

d) Learned Pruning Performance: To achieve a computationally efficient policy, we train Learned Pruning to map full garden observations from gardens with the plant types in Table II to prune levels. We simulate Variable Pruning on 10,000 gardens with randomized seed locations to collect prune level demonstrations. The network is trained with 800K demonstrations for 30 epochs with the Adadelta [40] optimizer and mean squared error loss. Table III summarizes results averaged across 20 test gardens withheld from the training dataset. Learned Pruning achieves comparable performance to Variable Pruning but is over 1000X faster in predicting $U(t)$ for days 20 to 70.

IX. Conclusion

This paper presents a physical polyculture farming testbed for estimating plant growth parameters and inter-plant companion effects. We use the estimated parameters to tune AlphaGardenSim 2.0 parameters, and developed an optimization algorithm that uses companion plant relations to generate a seed placement which yields high coverage and plant diversity. We trained a supervised-learned policy that is able to achieve high leaf coverage and plant diversity 1000X faster than a lookahead policy. In future work we will estimate stochastic models of growth parameters observed in the physical testbed and use these to optimize seed placements for subsequent growth cycles. This seed placement algorithm, learned plant phenotyping model, and learned irrigation and pruning models will be combined into a fully automated controller that will operate irrigation and pruning tools over multiple plant growth cycles.

Acknowledgements

This research was performed at the AUTOLAB at UC Berkeley in affiliation with the Berkeley AI Research (BAIR) Lab, and the CITRIS ”People and Robots” (CPAR) Initiative. This research was supported in part by the RAPID: Robot-Assisted Precision Irrigation Delivery Project (USDA 2017-67021-25925 under NSF National Robotics Initiative). The authors were supported in part by donations from Google, Siemens, Toyota Research Institute, Autodesk, Honda, Intel, Hewlett-Packard, a fellowship within the IFI programme of the German Academic Exchange Service (DAAD). We thank our colleagues who provided helpful feedback and suggestions, in particular Mary Power, Sarah Newman, Eric Siegel, Isaac Blankensmith, Maya Man, Christiane Paul, Charlie Brummer, Christina Wistrom, Grady Pierroz and Vishal Satish.

References

[1] S. J. Risch, "Intercropping as cultural pest control: prospects and limitations," *Environmental Management*, vol. 7, no. 1, pp. 9–14, 1983.

[2] T. E. Crews, W. Carton, and L. Olsson, "Is the future of agriculture perennial? imperatives and opportunities to reinvent agriculture by shifting from annual monocultures to perennial polycultures," *Global Sustainability*, vol. 1, 2018.

[3] S. Gliessman, M. Altieri *et al.*, "Polyculture cropping has advantages," *California Agriculture*, vol. 36, no. 7, pp. 14–16, 1982.

[4] M. Liebman, "Polyculture cropping systems," in *Agroecology*. CRC Press, 2018, pp. 205–218.

[5] S. E. Jorgensen and B. D. Fath, *Encyclopedia of ecology*. Newnes, 2014.

[6] F. Zhang and L. Li, "Using competitive and facilitative interactions in intercropping systems enhances crop productivity and nutrient-use efficiency," *Plant and soil*, vol. 248, no. 1-2, pp. 305–312, 2003.

[7] N. Bogie, R. Bayala, I. Diedhiou, R. Dick, and T. Ghezzehei, "Intercropping with two native woody shrubs improves water status and development of interplanted groundnut and pearl millet in the sahel," *Plant and soil*, vol. 435, no. 1-2, pp. 143–159, 2019.

[8] T. Tscharntke, Y. Clough, S. A. Bhagwat, D. Buchori, H. Faust, D. Hertel, D. Hölscher, J. Juhrbandt, M. Kessler, I. Perfecto *et al.*, "Multifunctional shade-tree management in tropical agroforestry landscapes–a review," *Journal of Applied Ecology*, vol. 48, no. 3, pp. 619–629, 2011.

[9] T. S. Rosenstock, D. Liptzin, K. Dzurella, A. Fryjoff-Hung, A. Hollander, V. Jensen, A. King, G. Kourakos, A. McNally, G. S. Pettygrove *et al.*, "Agriculture's contribution to nitrate contamination of californian groundwater (1945–2005)," *Journal of Environmental Quality*, vol. 43, no. 3, pp. 895–907, 2014.

[10] A. Mantovani. (2019) Pesticide risk assessment: European framework shows need for safer alternatives. [Online]. Available: https://www.openaccessgovernment.org/pesticide-risk-assessment/79226/

[11] D. Tilman, K. G. Cassman, P. A. Matson, R. Naylor, and S. Polasky, "Agricultural sustainability and intensive production practices," *Nature*, vol. 418, no. 6898, pp. 671–677, 2002.

[12] Y. Avigal, J. Gao, W. Wong, K. Li, G. Pierroz, F. S. Deng, M. Theis, M. Presten, and K. Goldberg, "Simulating polyculture farming to tune automation policies for plant diversity and precision irrigation," in *2020 IEEE 16th International Conference on Automation Science and Engineering (CASE)*. IEEE, 2020, pp. 238–245.

[13] J. Minchin. (2020) Romi: Robotics for microfarming. [Online]. Available: https://www.openaccessgovernment.org/romi-robotics-for-microfarming/80533/

[14] B. F. INC. (2020) Bowery farming. [Online]. Available: https://boweryfarming.com/

[15] J. S. Ken Goldberg. (1995) The telegarden. [Online]. Available: https://goldberg.berkeley.edu/garden/Ars/

[16] K. Goldberg, *The Robot in the Garden: Telerobotics and Telepistemology in the Age of the Internet*. Mit Press, 2001.

[17] M. Wiggert, L. Amladi, R. Berenstein, S. Carpin, J. Viers, S. Vougioukas, and K. Goldberg, "Rapid-molt: A meso-scale, open-source, low-cost testbed for robot assisted precision irrigation and delivery," in *2019 IEEE 15th International Conference on Automation Science and Engineering (CASE)*. IEEE, 2019, pp. 1489–1496.

[18] S. Fernando, R. Nethmi, A. Silva, A. Perera, R. De Silva, and P. W. Abeygunawardhana, "Ai based greenhouse farming support system with robotic monitoring," in *2020 IEEE REGION 10 CONFERENCE (TENCON)*. IEEE, 2020, pp. 1368–1373.

[19] T. Stomph, C. Dordas, A. Baranger, J. de Rijk, B. Dong, J. Evers, C. Gu, L. Li, J. Simon, E. S. Jensen *et al.*, "Designing intercrops for high yield, yield stability and efficient use of resources: Are there principles?" in *Advances in Agronomy*. Elsevier, 2020, vol. 160, no. 1, pp. 1–50.

[20] J. W. Jones, G. Hoogenboom, C. H. Porter, K. J. Boote, W. D. Batchelor, L. Hunt, P. W. Wilkens, U. Singh, A. J. Gijsman, and J. T. Ritchie, "The dssat cropping system model," *European journal of agronomy*, vol. 18, no. 3-4, pp. 235–265, 2003.

[21] P. Steduto, T. C. Hsiao, D. Raes, and E. Fereres, "Aquacrop—the fao crop model to simulate yield response to water: I. concepts and underlying principles," *Agronomy Journal*, vol. 101, no. 3, pp. 426–437, 2009.

[22] J. E. Whitman, H. Maske, H. A. Kingravi, and G. Chowdhary, "Evolving gaussian processes and kernel observers for learning and control in spatiotemporally varying domains: With applications in agriculture, weather monitoring, and fluid dynamics," *IEEE Control Systems Magazine*, vol. 41, no. 1, pp. 30–69, 2021.

[23] F. Gou, M. K. van Ittersum, and W. van der Werf, "Simulating potential growth in a relay-strip intercropping system: model description, calibration and testing," *Field Crops Research*, vol. 200, pp. 122–142, 2017.

[24] M. Tan, F. Gou, T. J. Stomph, J. Wang, W. Yin, L. Zhang, Q. Chai, and W. van der Werf, "Dynamic process-based modelling of crop growth and competitive water extraction in relay strip intercropping: Model development and application to wheat-maize intercropping," *Field Crops Research*, vol. 246, p. 107613, 2020.

[25] Y. Yu, "Crop yields in intercropping: meta-analysis and virtual plant modelling," Ph.D. dissertation, Wageningen University, 2016.

[26] FarmBot. (2020) Farmbot. [Online]. Available: https://farm.bot/

[27] T. B. Olaf Ronneberger, Philipp Fischer, "U-net: Convolutional networks for biomedical image segmentation," *arXiv preprint arXiv:1505.04597*, 2015.

[28] S. R. J. S. Kaiming He, Xiangyu Zhang, "Deep residual learning for image recognition," *arXiv preprint arXiv:1512.03385*, 2015.

[29] J. Deng, W. Dong, R. Socher, L.-J. Li, K. Li, and L. Fei-Fei, "Imagenet: A large-scale hierarchical image database," in *2009 IEEE conference on computer vision and pattern recognition*. Ieee, 2009, pp. 248–255.

[30] C. W. Whippo and R. P. Hangarter, "Phototropism: bending towards enlightenment," *The Plant Cell*, vol. 18, no. 5, pp. 1110–1119, 2006.

[31] D. Dietrich, "Hydrotropism: how roots search for water," *Journal of experimental botany*, vol. 69, no. 11, pp. 2759–2771, 2018.

[32] METER environment. [Online]. Available: https://www.metergroup.com/environment/

[33] B. B. Lin, M. H. Egerer, H. Liere, S. Jha, and S. M. Philpott, "Soil management is key to maintaining soil moisture in urban gardens facing changing climatic conditions," vol. 8, no. 1, p. 17565, number: 1 Publisher: Nature Publishing Group. [Online]. Available: https://www.nature.com/articles/s41598-018-35731-7

[34] P. G. Seeds. (2020) Pinetree garden seeds - vegetable collections. [Online]. Available: https://www.superseeds.com/

[35] K. Adamczewska-Sowińska and J. Sowiński, "Polyculture management: A crucial system for sustainable agriculture development," in *Soil Health Restoration and Management*. Springer, 2020, pp. 279–319.

[36] J. Parker, W. Snyder, G. Hamilton, and C. Rodriguez-Saona, "Companion planting and insect pest control," *Weed and Pest Control - Conventional and New Challenges*, pp. 1–30, 01 2013.

[37] A. L. Iverson, L. E. Marín, K. K. Ennis, D. J. Gonthier, B. T. Connor-Barrie, J. L. Remfert, B. J. Cardinale, and I. Perfecto, "Review: Do polycultures promote win-wins or trade-offs in agricultural ecosystem services? a meta-analysis," *Journal of Applied Ecology*, vol. 51, no. 6, pp. 1593–1602, 2014. [Online]. Available: https://besjournals.onlinelibrary.wiley.com/doi/abs/10.1111/1365-2664.12334

[38] S. Yogesh, S. Halikatti, S. Hiremath, M. Potdar, S. Harlapur, H. Venkatesh *et al.*, "Light use efficiency, productivity and profitability of maize and soybean intercropping as influenced by planting geometry and row proportion." *Karnataka Journal of Agricultural Sciences*, vol. 27, no. 1, pp. 1–4, 2014.

[39] W. Ren, L. Hu, J. Zhang, C. Sun, J. Tang, Y. Yuan, and X. Chen, "Can positive interactions between cultivated species help to sustain modern agriculture?" *Frontiers in Ecology and the Environment*, vol. 12, no. 9, pp. 507–514, 2014. [Online]. Available: https://esajournals.onlinelibrary.wiley.com/doi/abs/10.1890/130162

[40] M. D. Zeiler, "Adadelta: an adaptive learning rate method," *arXiv preprint arXiv:1212.5701*, 2012.

[41] K. Goldberg and R. Siegwart, *Beyond Webcams: an introduction to online robots*. MIT press, 2002.

[42] J. L. Harper *et al.*, "Population biology of plants." *Population biology of plants.*, 1977.

[43] T. Kijima, *Japanese Style Companion Planting*. Tuttle Publishing, 2020.